RSC Advances

ROYAL SOCIETY OF CHEMISTRY

www.rsc.org/advances

Graphene-decorated porous ceramics for efficient removal of Cr(VI)

Shi Wang, Wen Yang, Guohua Chen*

Department of Polymer Science & Engineering Huaqiao University,

Xiamen 361021, People' s Republic of China

*Corresponding Author. Tel.: +86-592-6166296; fax: +86-592-6166296.

E-mail: hdcgh@hqu.edu.cn.

Abstract: Porous ceramics (such as activated alumina (AA)) is a common adsorbent material in water purification. Its purifying capacity can be greatly improved through modification of porous ceramics. In this paper, a facile method has been established to prepare graphene-decorated porous ceramics (GDPC) material. Citric acid (CA) was absorbed into the inner surface of the porous ceramics and transformed to graphene via sintering. The as-prepared material showed excellent adsorption capacity for chromium (Cr(VI)) over a wide range of pH (2 to 10) compared with the blank sample. The maximum uptake capacity for Cr(VI) exceed 699.43 mg g^{-1}. UV and ICP-OES test indicated that chromium ions in aqueous solution were completely removed via the GDPC. Thus the GDPC could be a potential adsorbent for the environmental cleanup, especially for the chromium-contained wastewater disposal.

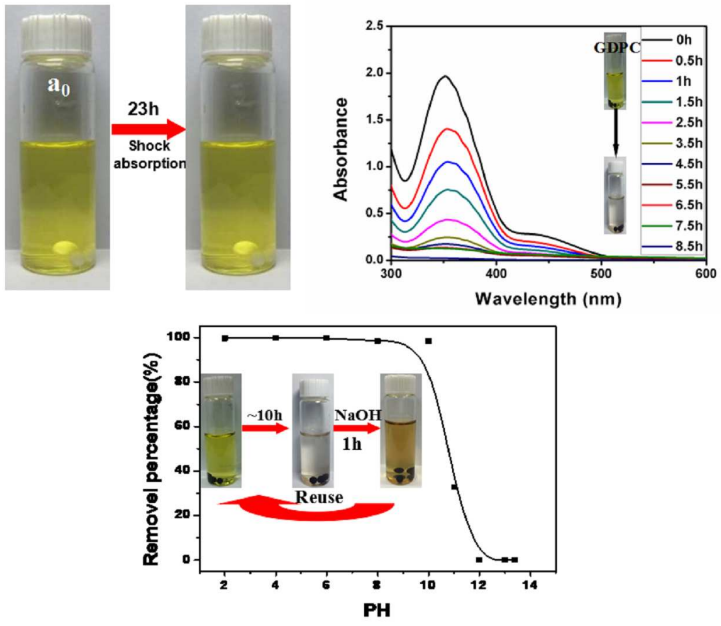

Keywords: graphene porous ceramics composite water purification citric acid

1 Introduction

Nowadays, hexavalent chromium (Cr(VI)) is one of the most poisonous substances threatening human's subsistence and environmental sustainability. It is reported that chromium coming from leather tanning, mining operation, electroplating, and pigment manufacturing and so on is the second most abundant inorganic groundwater contaminant at hazardous waste sites.[1,2] The major technologies for the removal of Cr(VI) are reverse osmosis,[3] ion exchange,[4] electro-chemical precipitation[5] and adsorption,[6,7] etc. Among these methods available for Cr(VI) removal in aqueous solution, adsorption is considered as the most efficient and economical one.[8, 9]

The activated carbon derived from various sources has been used for the adsorption of chromium.[10] However, the problem is that its best adsorption performance is shown in a narrow pH range.[11] Its uptake ability is also highly limited.[12] Activated alumina (AA), a kind of porous ceramics applied to the water purification, is also circumscribed in the field of chromium adsorption. For instance, Bishnoi et al. reported that the maximum removal of Cr(VI) occurred at pH 4 by AA and the adsorption capacity decreased significantly in other pH range.[13] The phenomenon was also demonstrated by Mor et al..[14] There are reports illustrating that not only AA shows the unsatisfactory adsorption behavior in Cr(VI) , but also other materials,[15-19] such as polyaniline coated ethyl cellulose.

In recent years, graphene and graphene-based composites are increasingly important in water purification. For example, Han et al. Fabricated a ultrathin

graphene nanofiltration membrane for water purification.[20] Zhu et al. reported that graphene decorated with core@double shell nanoparticles was synthesized for fast Cr(VI) removal.[21] Kumar et al. also prepared a novel amine impregnated graphene oxide composite as an effective adsorbent for Cr(VI) removal.[22] By now, graphene can be produced through Peel-off graphite, chemical vapor deposition, unzipping carbon nanotubes, templating and organic synthesis, reduction of graphene oxide, etc.[23] All the methods above have their own advantages and disadvantages according to each application. Recently, using organic molecules and polymer as graphene/graphite precursor is catching wide interests,[24-29] since these green methods have the superiority of flexibility. It seems that most organic materials can be turned to graphene under specific conditions. For example, Seo et al. reported that a range of natural precursors (honey, milk, methane, butter, and table sugar) in different physical states (gas, liquid, and solid) and chemical compositions were transformed to graphene under plasma condition.[30] Ruiz-Hitzky et al. revealed that sucrose and gelatin could be assembled to silica and silicate porous solids, and transformed to graphene-like material through thermal treatment.[31] Gupta et al.[32] and Sreeprasad et al.[33] prepared graphene-sand composite adsorbent materials using sugar and asphalt as carbon sources at the condition of heating, respectively. More interestingly, Dong et al.[34] demonstrated that CA can be transformed to graphene oxide through directly pyrolyzing.

In this paper, a simple strategy was proposed to synthesize the graphene-decorated granule porous AA. This modified AA showed a significantly

improved adsorption capacity for Cr(VI) over a wide range of pH (2 to 10). Experiments confirmed that graphene-decorated porous ceramics (GDPC) showed a strong adsorption capacity for chromium ions in aqueous solution. The maximum adsorption capacity was as high as 699.43 mg g^{-1}.

2 Materials and method

Materials, the optimal sintering time for preparation of GDPC and the details of preparation for each concentration of hexavalent chromium containing solution are given in supplementary data 1. The process of preparation of GDPC starting from CA and porous ceramics (AA) is shown in Fig. 1. The GDPC was obtained in situ creation. Firstly, blank AA was washed repeatedly and then dried in vacuum oven for 48 h. 100 g CA monohydrate (the carbon source) was dissolved in 500 ml distilled water and denoted as C_1. Secondly, half of the solution was double diluted by distilled water and named as C_2 (C_2=C_1/2). Using the same method, C_3 (C_3=C_2/2) was got. Thirdly, 60g washed and dried AA were heated at 500 ℃ for 10 min to remove the air in porous ceramics and poured into the three different concentrations of CA solution (250 ml) for 24 h, respectively. Fourthly, the CA-coated AA (a_1, a_2, a_3) was dried in oven and heated in the muffle at 500 ℃ for 15 min without any special treatment. The fetched out black sample was named as GDPC, and the three different coating ratios GDPC were labeled as GDPC(a_1), GDPC(a_2), GDPC(a_3) (GDPC(a_1), GDPC(a_2), GDPC(a_3) represent the carbon loading of 1.37%, 0.69%, and 0.35%, respectively. The carbon loading is calculated by the constant weight method and the detailed computational method is presented in supplementary data 2). For comparison,

AA was treated as the aforementioned procedure without any CA addition, and the sample was marked as a_0.

Fig. 1. The progress of preparation of GDPC (upper frame).

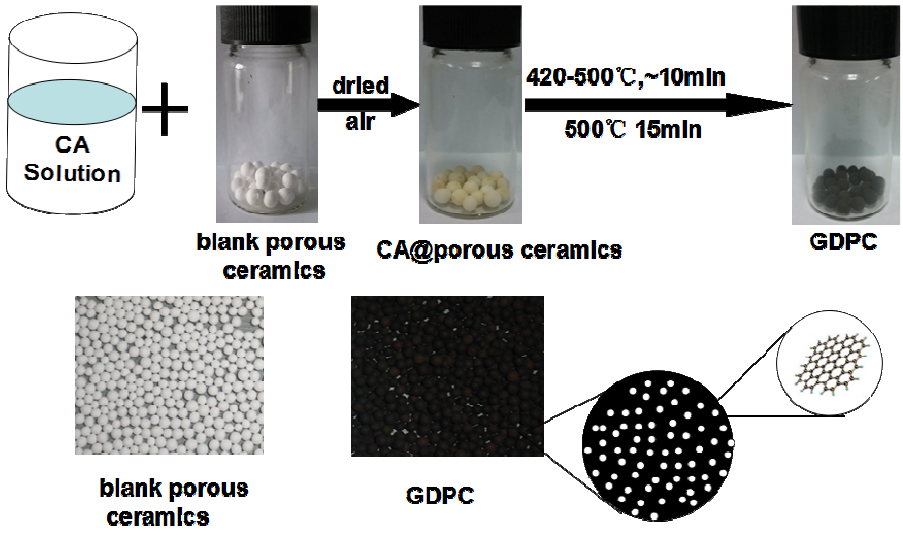

Photographs of pristine granule porous ceramics (AA) and GDPC (Lower frame).

2.1. Adsorption Experiments

a_0, GDPC(a_1), GDPC(a_2), GDPC(a_3) were evaluated for their ability to remove Cr(VI) from water. A certain amount of adsorbent was added to 10 ml of corresponding hexavalent chromium-containing solution and followed by shaking (100 rpm) at room temperature for 10 h. The concentration of residual Cr(VI) in the supernatant was determined by UV-vis spectrophotometer (UV-1600, Beijing Rayleigh Analytical Instruments) at 350 nm.[35, 36] In order to test whether the treated solution had trace residual chromium ions, inductively coupled plasma optical emission spectrometer (ICP-OES, Optima 7000DV) was used. Except kinetics, all other studies were conducted in triplicate. The optimum dosage choosing of GDPC is

given in supplementary data 3.

2.2. Materials characterization

The morphologies of AA and GDPC(a_1) were characterized by field emission scanning electron microscopy (FESEM, LEO1530). Elemental analysis and elemental mapping studies of samples were carried out with an energy dispersive spectrometer (EDS) attached to the FESEM. Morphology of the graphene loaded in GDPC(a_1) was characterized by a transmission electron microscopy (TEM,JEM-2010 JEOL). Raman spectra were recorded with a He-Ne Laser (532 nm) as the excitation source by Labram spectrometer (Super LabRam II system), and used to analyze GDPC(a_1) and G_{CA} (G_{CA} represented CA prepared under the same condition as GDPC but without the addition of AA). X-ray powder diffraction (XRD) measurements were obtained by a D8-Advance instrument, using Cu-Kα radiation (λ=1.54178 Å). The X-ray photoelectron spectroscopy (XPS) measurement was performed in the Thermo ESCALAB 250XI instrument using a monochromatic Al Ka (hv=1486.6 eV, power=150 W) radiation to determine the valence state of chromium. Fourier transformed infrared (FT-IR) spectroscopy was performed using a Nicolet Nexus FT-IR spectrometer over a range from 400 to 4000 cm^{-1}. N_2 adsorption/desorption experiments were carried out using a Quantachrome Nova 1200e type automatic specific surface and pore analyzer. The pH measurements were carried out using a digital pH meter (Lei-ci pHS-2F).

3. Results and discussion

3.1. Characterization of GDPC

The surface of a_0 is composed of many granules (about 2 μm) which shows the microstructure of AA (Fig. 2A). However, as shown in Fig 2B, some sheet-like structure emerges after the sintering of the ceramics which have been soaked in CA solution , and the average diameter of the sheet is about 10 μm. Moreover, the sheets are surrounded by AA particles, indicating the high surface energy of the generated sheet-like structure. It is most likely that the creation of these sheets is attributed to the completely carbonization of CA, which is the method to produce graphene from some organic molecules in previous reports.[31-34]

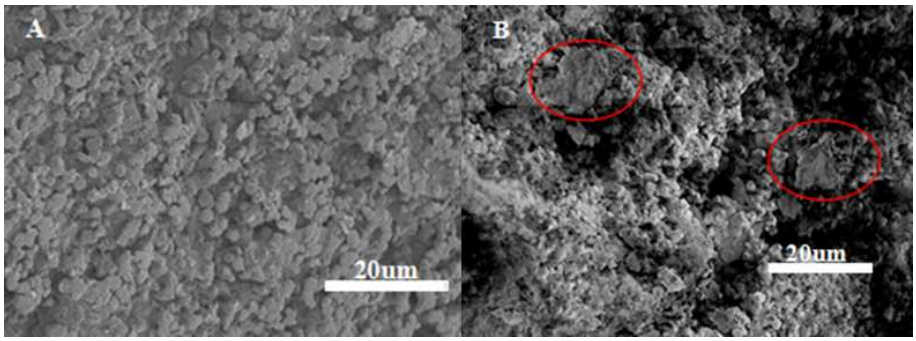

Fig. 2. (A and **B)** SEM images of a_0 and GDPC(a_1).

The graphenic characteristic peak (002) appears at around ~23° in XRD spectrum of G_{CA} (Fig. 3A), further indicating the totally carbonization of pure CA. Compared with a_0, almost no new feature appears in GDPC(a_1)'s XRD measurement, probably because of the low carbon loading. In this case, the graphenic material was collected by N-Methyl-2-pyrrolidone (NMP) from GDPC(a_1) (abbreviated as GDPC(a_1)-NMP), and then the characteristic peak at ~23° reappeared. It suggests that the similar carbonization of the CA is also occurred, this can be visually observed in TEM photograph (Fig. 3B). TEM image shows that the graphenic materials are

composed of single- and multi-layer sheet structures, and many edges present wrinkly state.

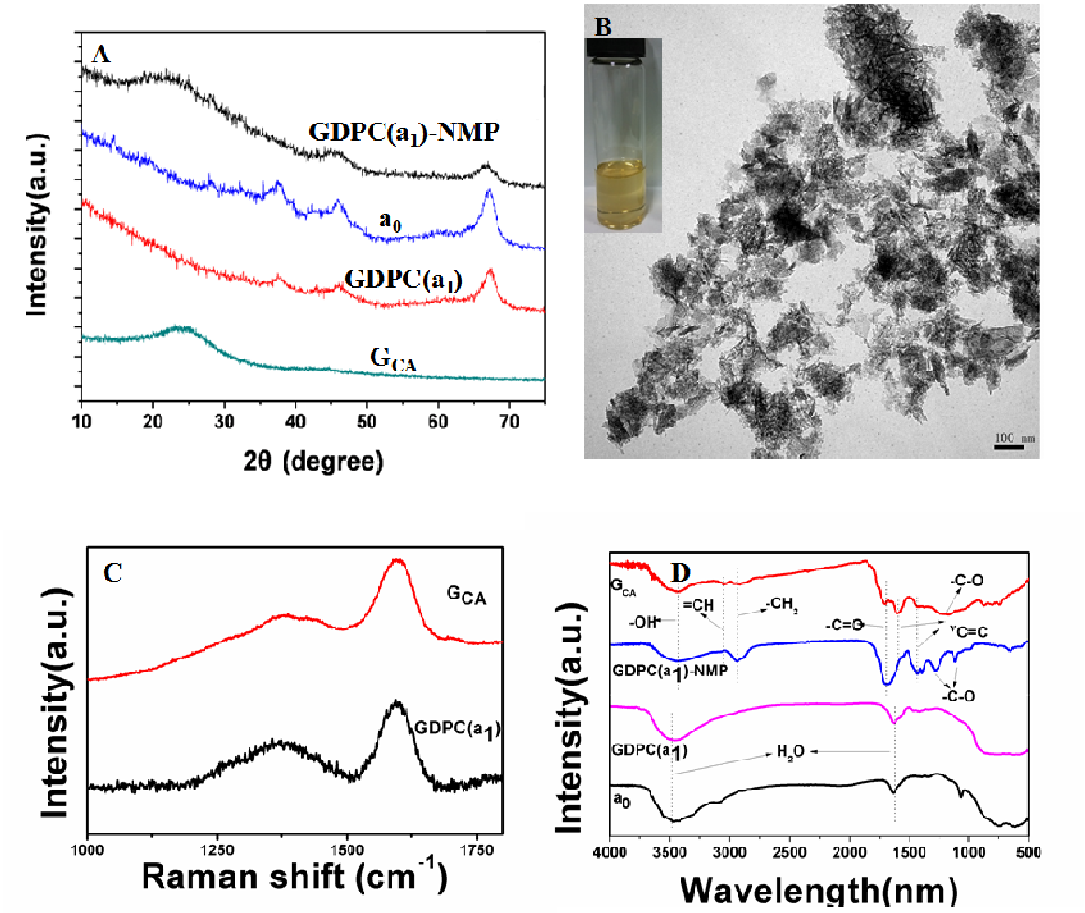

Fig. 3. (**A**) XRD spectra of GDPC(a_1)-NMP, a_0, GDPC(a_1), and G_{CA}. (**B**) TEM image of graphenic material loaded in AA dissolved by NMP, and inside of (B) was photograph of the graphene dispersion liquid. (**C**) Raman spectra of sample G_{CA} and GDPC(a_1). (**D**) IR spectra of G_{CA}, GDPC(a_1)-NMP, GDPC(a_1) and a_0.

The complicated information of graphene, such as the defects and crystal structure, can be effectively collected by Raman spectrum. Highly similar to graphene, Fig. 3C shows that both GDPC(a_1) and G_{CA} have a prominent G band and a much weaker D band at 1594 and 1397 cm^{-1}, respectively. The intensive G band suggests

complete graphitization of CA, while the D band indicates some defects in the synthesized analogues of graphene. According to the previous report,[37] the edge detects of graphene can be considered as reactivity points which are very easy to bond with polar groups. FTIR test in Fig. 3D indicates that G_{CA} and GDPC(a_1)-NMP present the characteristic absorption peak of the same functional groups.

3.2. Batch adsorption experiments

3.2.1. The effect of initial concentration of Cr(VI) and adsorption ability of GDPC

Fig. 4A shows that the uptake ability of carbon on GDPC(a_1) to Cr(VI) at concentrations of 62.5, 125, 250 ppm are 178.69, 361.46, 598.83mg g^{-1}, respectively. UV-vis spectra in Fig. 4B presents a very low Cr(VI) content in the solution after the solution was treated by GDPC under the same conditions and the bar charts in Fig. 4B indicate that the adsorption capacity of carbon on GDPC(a_1), GDPC(a_2) and GDPC(a_3) are 317.8, ≥ 354.78 and ≥ 699.43 mg g^{-1}, respectively. However, the adsorption capacity of a_0 for Cr(VI) is 0 mg g^{-1} under the same conditions of GDPC (the adsorption capacity of GDPC are more than 317.8 times higher than that of a_0 under this condition, as shown in Fig. 4B). In fact, chromium ions can be 100% removed after adding a little bit of GDPC(a_1), which is confirmed by ICP-OES test (When the chromium(VI) ion concentration in the solution is extreme low, ICP-OES can effectively detect the exact residual chromium concentration[35]). In this study, the adsorbent capacity of the carbon on GDPC is also compared with different kind of activated carbon,[38-43] as shown in table 1. The result indicates that GDPC is relatively

more superior.

The image of EDS of Fig. 4C reveals that potassium dichromate is adsorbed on GDPC(a_1), as feature elements Cr and K appear in the map (For comparison, the EDS map of a_0 is sent in supplementary data 4, Fig. S4). The N_2 adsorption/desorption

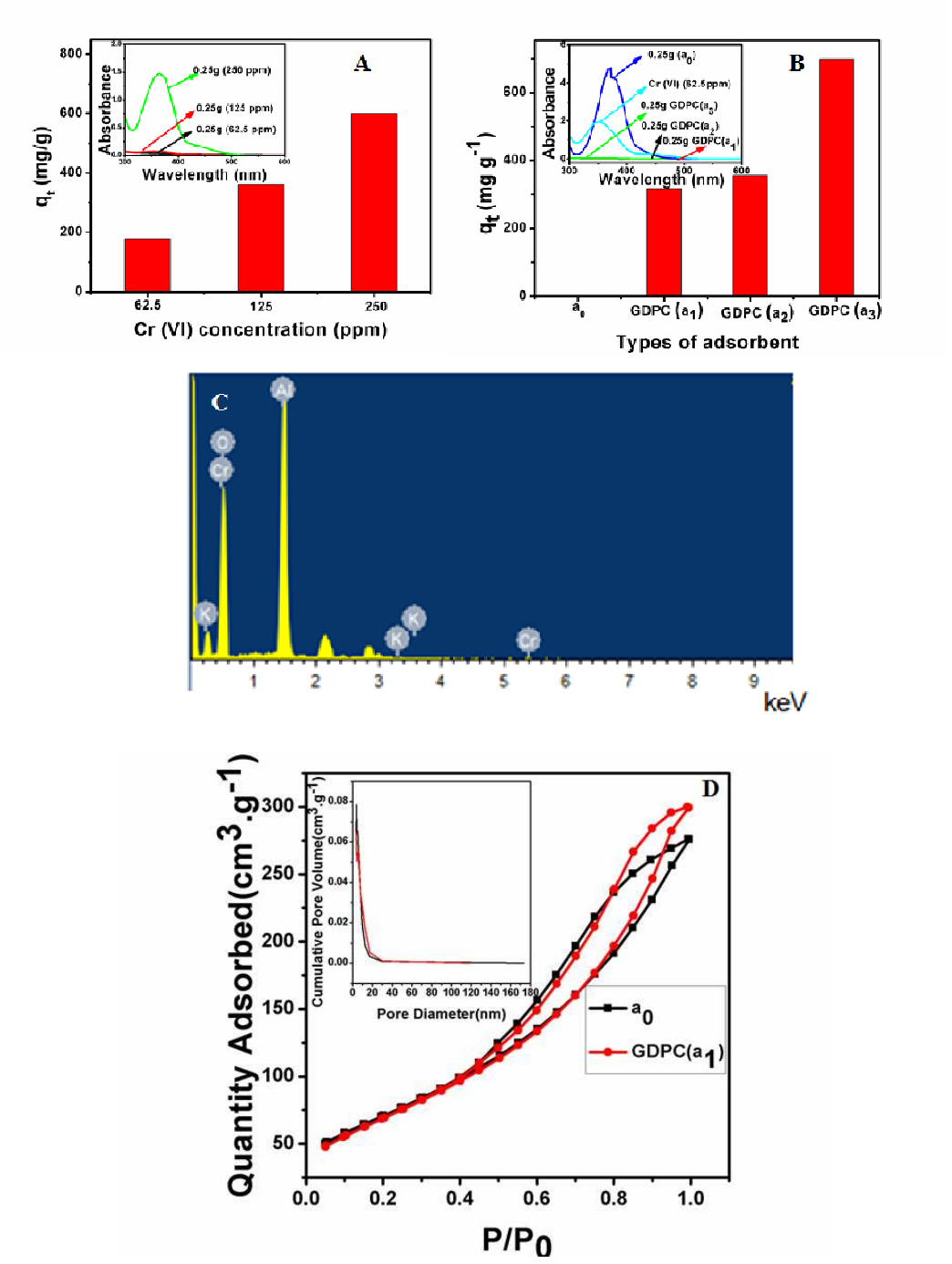

Fig.4. (A) Absorption capacity of Cr(VI) on GDPC(a_1) of different concentration and the inside of (A) is the corresponding UV-Vis spectra (Adsorption condition: quality of GDPC(a_1)= 0.25 g, initial concentration of Cr (VI)= 62.5 ppm, 125 ppm, 250 ppm (10 ml), room temperature, pH= 5.08, stirring speed = 100 rpm, contact time= 8.5 h). **(B)** The adsorption ability of GDPC(a_1), GDPC(a_2), GDPC(a_3) compared with a_0 at the same dose (0.25 g) and the inside of (B) is the corresponding UV-Vis spectra. (Adsorption condition: initial concentration of Cr (VI)= 62.5 ppm (10 ml), room temperature, pH=5.08, stirring speed= 100 rpm, contact time= 8.5 h). **(C)** EDS photograph of GDPC(a_1) after adsorbing chromium ions, the content of chromium was 8.31% on GDPC(a_1). **(D)** N_2 adsorption/desorption isotherm for mesoporous a_0 and GDPC(a_1).

isotherms for a_0 and GDPC(a_1) are shown in Fig. 4D, the two samples both have a narrow pore size distribution with an average pore diameter of 3.822 and 3.422 nm, a high surface area of 261.157 and 257.086 $m^2 g^{-1}$, and a high pore volume of 0.404 and 0.441 $cm^3 g^{-1}$, respectively. Compared with AA, the GDPC shows little change in the surface area, but its adsorption ability is totally different. Thus the cause for the great improvement of modified AA in the adsorption ability should be attributed to the decoration of defective graphene (Fig. 3C and D). The use of porous ceramics as the framework can carry graphene and prevent the agglomeration of graphene. Moreover, the graphene sheets that grow on porous ceramics are nanosheets (as shown in Fig. 3B), which can greatly increase the specific surface area of graphene, thus results in the increased adsorption ability.

3.2.2. The effect of pH

Fig. 5A shows that Cr(VI) can be maximally removed by a_0 at pH 2, only part of Cr(VI) can be removed at pH between 1 and 2. When the pH is higher than 2, the adsorption capacity of AA is in steep decline. The reason has been given by other researchers, as a large number of H^+ ions can neutralize the negatively charged adsorbent surface thereby reducing hindrance to the diffusion of dichromate ions at low pH.[13] With the increase of pH, the degree of protonation of the surface decreases gradually and hence adsorption is declined (the competition between OH^- and chromate ions (CrO_4^{2-}) at high pH should also been concerned).[14] However, GDPC(a_1)

Table 1. Comparison of the maximum adsorption capacities for Cr(VI) of carbon on GDPC (Adsorption condition: quality of GDPC= 0.25 g, initial concentration of Cr (VI) = 62.5 ppm (10 ml), room temperature, pH= 5.08, stirring speed = 100 rpm, contact time = 8.5 h) with other different kinds of activated carbon.

Adsorbents	pH	Adsorption capacity of carbon (mg g^{-1})	References
Activated carbon (PAC)	2.5-3.0	145	11
Activated carbon (Palm kernel fiber)	3	19.1	38
Activated carbon (peanut shell)	4	~15	39
Activated carbon (PAC)	2	390	40
Activated carbon (ACF)	-	40	41
Activated carbon (Rubber wood sawdust)	2	65.78	42
Activated carbon (GAC-Filtrasorb 400)	2	53.19	43
GDPC(a_1)	5.08	317.87	This study
GDPC(a_2)	5.08	~354.78	This study
GDPC(a_3)	5.08	~699.43	This study

shows an excellent performance compared with a_0 in a wide pH range under the same conditions (Fig. 5B). The removal percentage of 99.7%, 99.8%, 99.9%, 98.4%, 98.4% is reached by GDPC(a_1) at pH 2, 4, 6, 8, 10, respectively. The reason of the great

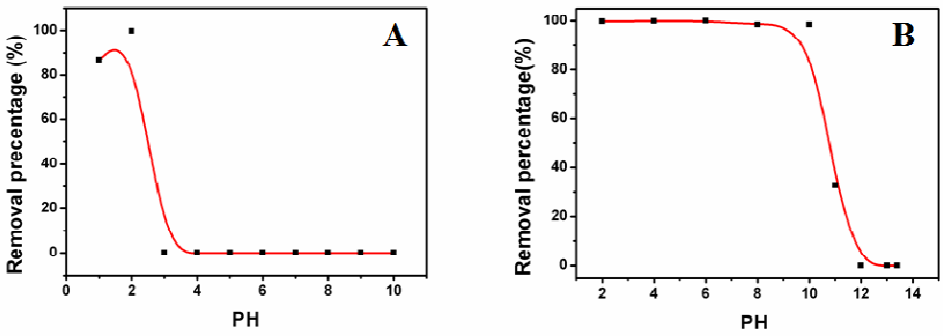

Fig.5. Effect of solution pH on the adsorption of Cr(VI) on a_0 (Adsorption condition: quality of a_0= 0.25 g, initial concentration of Cr(VI)= 62.5 ppm (10 ml), room temperature, stirring speed=100 rpm, contact time= 8.5 h) **(A)** and **(B)** GDPC(a_1) (Adsorption condition: quality of GDPC(a_1)= 0.25 g, initial concentration of Cr (VI)= 62.5 ppm (10 ml), room temperature, stirring speed=100 rpm, contact time=8.5 h).

performance of GDPC might be as follows: Hexavalent chromium may exists as chromate (CrO_4^{2-}), dichromate ($Cr_2O_7^{2-}$), or hydrogen chromate ($HCrO_4^-$), which particular depends on the pH of the aqueous solution. The following equation presents the equilibrium relationship between the different chromium anions.

$$2CrO_4^{2-} + 2H^+ \longleftrightarrow (2HCrO_4^-) \longleftrightarrow Cr_2O_7^{2-} + H_2O \quad \textbf{(1)}$$

It is believed that the GDPC can adsorbs Cr(VI) in such a wide pH range (2-10) is because of the surface of GDPC carries positive charges. When at low pH, eqn (5) is driven to the right-hand side, resulting in the formations of hydrogen chromate and dichromate which have less affinity for the carbon modified adsorbent in relation to

the chromate ion. On the contrary, at high pH (For example, pH> 10), the formation of $Cr(OH)_3$ greatly limit GDPC to removal of Cr(VI). The chromium anions may also polymerize and grow at low pH and thus decreasing the accessibility of chromium species to adsorption sites. Moreover, the competition between OH^- and chromate ions (CrO_4^{2-}) at high pH should also been concerned.[44]

3.2.3. Kinetic study

Batch adsorption experiments were performed to evaluate the adsorption ability of GDPC(a_1), GDPC(a_2), GDPC(a_3). Fig. 6A indicates that the intensity of absorption peak at 350 nm corresponding to the concentration of Cr(VI) decreases almost uniformly and then slows down at the same time interval. The reason might be that the number of unoccupied adsorption sites on GDPC decreases over time, then the system reaches pseudo equilibrium in 8.5 h (UV/vis data of GDPC(a_2), GDPC(a_3) are shown in supplementary data Fig. S5). This is consistent with Fig. 6B, which shows the uptake ability (mg g^{-1}) as a function of time. Furthermore, the kinetic curves are almost overlapped, further confirming the great adsorption capacity of GDPC(a_2), GDPC(a_3) to Cr (VI).

The experimental data was fitted by two well-known adsorption kinetic models, pseudo-first-order Lagergren model[45] and pseudo-second-order model.[46] The equations of the pseudo first-order model and pseudo-second-order model were represented as follows:

$$\log(q_e-q_t)=\log q_e-k_1t/2.0303 \quad (2)$$

Where q_t and q_e are the amounts of target pollutants adsorbed (mg g^{-1}) at time t (h)

and equilibrium. k_1 is the Lagergren rate constant of adsorption, and can be calculated from the slope of the plot of $\log(q_e-q_t)$ versus t.

Pseudo-second-order model can be expressed as follows:

$$t/q_t=1/k_2q_e^2+t/q_e \quad (3)$$

Where k_2 is the rate constant of adsorption, q_e and k_2 can be determined from the slope and intercept of the plot obtained by plotting t/q_t versus t. Fig. 6C and D give the linear fitting of pseudo-first-order model and pseudo-second-order model of the Cr(VI) adsorption on GDPC(a_1), GDPC(a_2), GDPC(a_3), respectively. The values of kinetic parameters are shown in supplementary data 6. Compared with pseudo-first-order model, the higher correlation coefficient and the much better agreement of the experiment and calculated q_e of pseudo-second-order model both suggested that the pseudo-second-order model is more appropriate to describe the system.

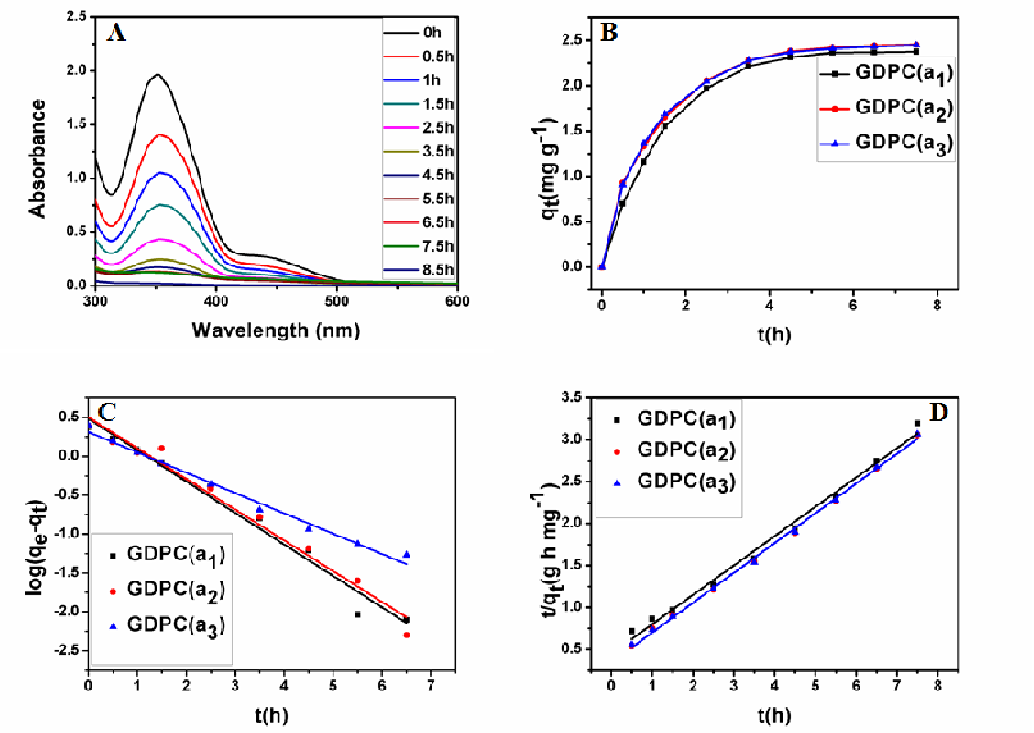

Fig. 6. (A) Kinetic study of the adsorption of Cr(VI) on GDPC(a_1) in a batch experiment and **(B)** the influence of contact time on the removal of Cr(VI). **(C)** pseudo-first-order model and **(D)** pseudo-second-order model of Cr(VI) adsorption on GDPC(a_1), GDPC(a_2), GDPC(a_3). (Adsorption condition: quality of GDPC(a_1)= 10 g, initial concentration of Cr (VI)= 62.5 ppm (400 ml), room temperature, pH= 5.08, stirring speed= 100 rpm, contact time= 8.5 h)

3.2.4. Adsorption isotherms

In this study, GDPC(a_1) was used to analyze its adsorption behavior of Cr(VI), both the Langmuir and Freundlich models[47, 48] were evaluated to simulate Cr(VI) adsorption isotherms. If the adsorbent has an ideal homogeneous adsorption surface with all the adsorption sites having the same sorption energy independent of surface coverage, the Langmuir model will be fitted. The equation of Langmuir isotherm is as follows:

$$C_e/q_e=C_e/q_{max}+1/(q_{max}\,k_L) \quad (4)$$

Where k_L is a Langmuir constant related to the affinity of the binding sites and energy of adsorption (L g^{-1}), q_{max} is the maximum removal performance (mg g^{-1}) and C_e is the equilibrium concentration of the solution (mg L^{-1}).

A heterogeneous adsorption surface of adsorbent can use Freundlich isotherm model to analyze. The equation is commonly expressed as follows:

$$\ln q_e=\ln k_F+ \ln C_e/n \quad (5)$$

Where 1/n is an empirical parameter related to adsorption intensity, and k_F is a Freundlich constant related to adsorption ability (L g^{-1}).

Fig. 7 presents the equilibrium isotherms for Cr(VI) adsorbed by GDPC(a_1). q_{max}, relating to the constants and the correlation coefficients involved in the two isotherm models are summarized in table 2. The isotherms parameters in table 2 indicate that the Langmuir model fitted the Cr(VI) adsorption isotherm better (such as the Langmuir model shows better correlation (R^2=0.9985) than the Freundlich model R^2=0.8754). Moreover, the n value is 8.9286 for the absorption of Cr(VI). Again, it indicates that the modified porous ceramics exhibits a highly efficient adsorption ability.

Table 2. Isotherm parameters for the adsorption of Cr(VI) on GDPC.

Sample	Target pollutant	Langmuir			Freundlich		
		Adsorption capacity (q_{max}) of carbon (mg g^{-1})	k_L (L g^{-1})	R^2	k_F (L g^{-1})	n	R^2
GDPC(a_1)	Cr(VI)	317.87	3.0130	0.9985	4.4838	8.9286	0.8754

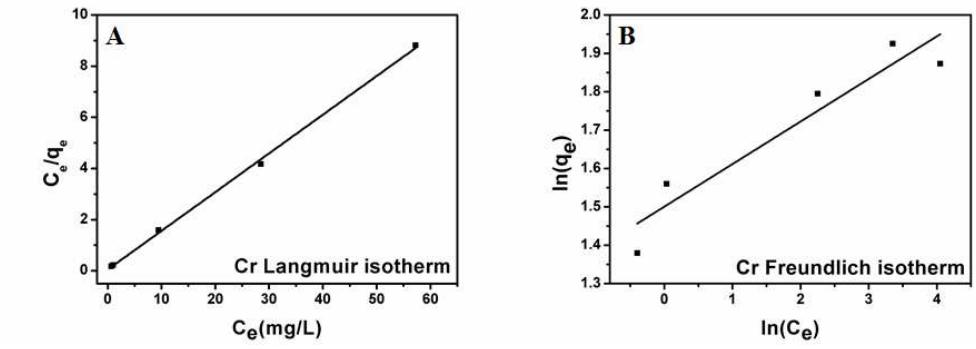

Fig. 7. The equilibrium isotherm for Cr(VI) adsorbed by GDPC (a_1), **(A)** the Langmuir isotherm and **(B)** the Freundlich isotherm. (Adsorption condition: quality of GDPC(a_1)= 0.25 g, initial concentration of Cr (VI)= 100 ppm, 120 ppm, 160 ppm, 200ppm, 220ppm (10 ml), room temperature, pH= 5.08, stirring speed= 100 rpm, contact time= 8.5 h)

3.2.5. Mechanism analysis and adsorption-desorption cyclic study

The valence state of chromium bound on GDPC can effectively reveal the mechanism of Cr(VI) and GDPC. XPS study shown in Fig. 8A presents the spectra of chromium from the GDPC after adsorption. The Cr(2p3/2) peak that is located at 580.6 ev contributes to Cr(VI)[49] which suggests that there is no change in the valence of the chromium after adsorption. Fig. 8B shows that the Cr(VI) containing GDPC(a_1) can be desorbed by NaOH solution, then receiving a chromium ion solution with deep yellow about 1 h later. It suggests that there is a comparatively weak bond existing between the Cr(VI) and GDPC. Thus far, the main adsorption mechanism of Cr(VI) onto GDPC can be suggested to be physical interactions, such as, electrostatic attraction and Van der Waals' force. In addition, Fig. 8B also reveals that GDPC could

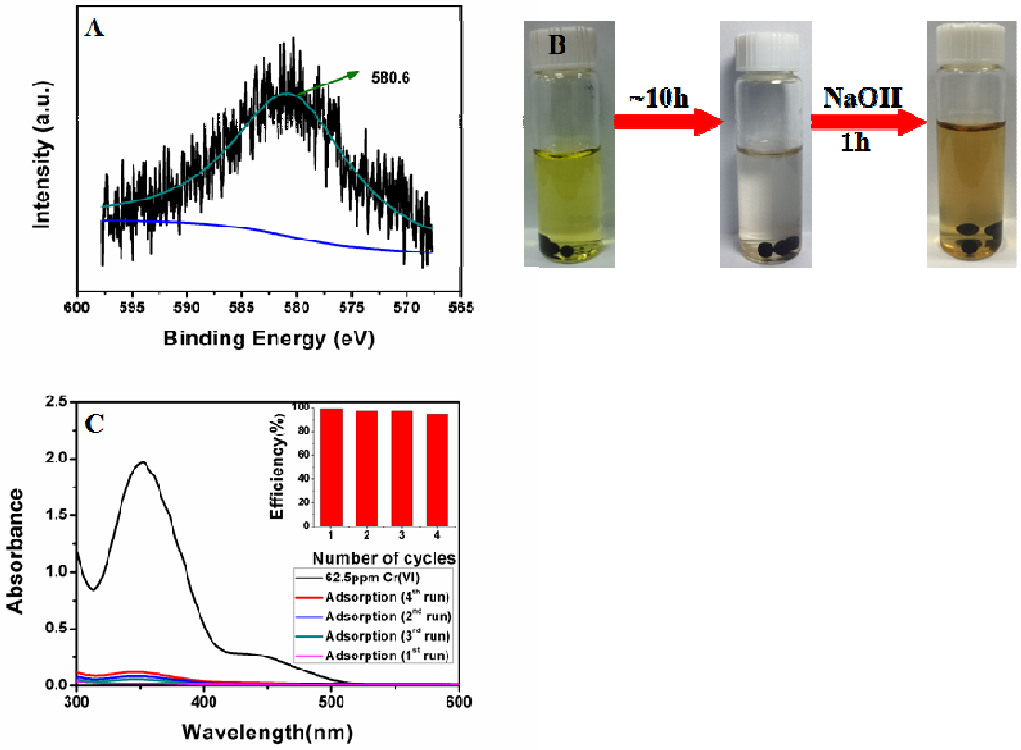

Fig. 8. (A) Cr 2p spectrum of the Cr-laden GDPC(a_1). **(B)** Desorption of Cr(VI) by

NaOH solution (The concentration of NaOH=1 mol/L (10 ml), the quality of GDPC(a_1)=0.25 g, room temperature, stirring speed= 100 rpm, contact time= 8.5 h) and **(C)** the ability of reuse of GDPC(a_1) for four consecutive adsorption cycles and efficiency bar (The concentration of NaOH= 1 mol/L (10 ml), the quality of GDPC(a_1)= 0.25 g, initial concentration of Cr (VI)= 62.5 ppm, room temperature, stirring speed = 100 rpm, contact time = 8.5 h).

be reused in water purification. As shown in Fig. 8C, after four times of adsorption-desorption cyclic, the removal percentage of GDPC(a_1) still remains as high as 94.49%.

4. Conclusions

In summary, a novel graphene-decorated porous ceramics has been fabricated by a facile strategy. Citric acid(CA), as the carbon precursor, was adsorbed to the inner surface of the porous ceramics (AA) and transformed to graphene via sintering, receiving the graphene-decorated AA. The as-prepared material has excellent adsorption capacity of chromium (Cr(VI)) in a wide pH range (2 to 10) compared with those of blank sample and activated carbon. The maximum uptake capacity of graphene in GDPC was more than 699.43 mg g^{-1} for Cr(VI). Moreover, the strong reused ability of the material has been demonstrated. Such a high adsorption capacity and the reusable ability illustrate the potential application of GDPC in water purification industry.

Notes

The authors declare no competing financial interest.

Acknowledgements

This work was funded by Natural Science Foundation of China (51373059) and Science Foundation of Fujian Province (2013H6014) and Science Foundation of Xiamen (3502Z20143044) and Science and technology innovation team of Huaqiao University (Z14X0046).

References

[1] W. T. Yu, L. Y. Zhang, H. Y. Wang and L. Y. Chai, J. Hazard. Mater., 2013, 260789–795.

[2] L. Zhou, H. P. Deng, J. l. Wan, J. Shi and T. Su, Appl. Surf. Sci., 2013, 283, 1024–1031.

[3] R. K. Goyal, N. S. Jayakumar and M. A. Hashim, J. Hazard. Mater., 2011, 195, 383–390.

[4] S. Rengaraj, C. K. Joo, Y. Kim and J. Yi, J. Hazard. Mater., 2003, 102, 257–275.

[5] N. Kongsricharoem and C. Polprasert, Water Sci. Technol., 1996, 34, 109.

[6] Y. Zhao, J. R. Peralta-Videa, J. R. Lopez-Moreno, M. Ren, G. Saupeand, J. L. Gardea-Torresdey, Environ. Sci. Technol., 2011, 45, 1082.

[7] D. Zhang, S. Y. Wei, C. Kaila, X. Su, J. Wu, A. B. Karki, D. P. Young and Z. H. Guo, Nanoscale, 2010, 2, 917–919.

[8] G. Gollavelli, C. C. Chang and Y. C. Ling, ACS Sustainable Chem. Eng., 2013, 1, 462–472.

[9] S. E. Bailey, T. J. Olin, R. M. Bricka and D. D Adrian, Water Res., 1999, 33, 2469 –2479.

[10] D. Mohan and C. U. PittmanJr., J. Hazard. Mater., 2006, 137, 762–811.

[11] D. C. Sharma and C. F. Forster, Water S.A., 1996, 22, 153–160.

[12] M. Owlad, M. K. Aroua, W. A. W. Daud and S. Baroutian, Water Air Soil Pollut., 2009, 200, 59–77.

[13] N. R. Bishnoi, M. Bajaj, N. Sharma and A. Gupta, Bioresour. Technol., 2004, 91, 305–307.

[14] S. Mor, K. Ravindra and N. R. Bishnoi, Bioresour. Technol., 2007, 98, 954–957.

[15] M. Owlad, M. K. Aroua and W. M. A. W. Daud, Bioresour. Technol., 2010, 101, 5098–5103.

[16] B. Qiu, C. X. Xu, D. Z. Sun, H. Yi, J. Guo, X. Zhang, H. L. Qu, M. Guerrero, X. F. Wang, N. Noel, Z. P. Luo, Z. H. Guo and S. Y. Wei, ACS Sustainable Chem. Eng., 2014, 2, 2070 −2080.

[17] L. Zhou, H. P. Deng, J. L. Wan, J. Shi and T. Su, Appl. Surf. Sci., 2013, 283, 1024–1031.

[18] H. Jabeen, V. Chandra, S. Jung, J. W. Lee, K. S. Kim and S. B. Kim, Nanoscale, 2011, 3, 3583–3585.

[19] J. H. Chen, H. T. Xing, H. X. Guo, W. Weng, S. R. Hu, S. X. Li, Y. H. Huang, X. Sun and Z. B. Su, J. Mater. Chem. A , 2014, 2, 12561.

[20] Y. Han, Z. Xu and C. Gao, Adv. Funct. Mater. 2013, 23, 3693–3700.

[21] J. H. Zhu, S. Y. Wei, H. B. Gu, S. B. Rapole, Q. Wang, Z. P. Luo, N. Haldolaarachchige, D. P. Young and Z. H. Guo, Environ. Sci. Technol. 2011, 46, 977−985.

[22] A. S. K. Kumar, S. S. Kakanb and N. Rajesh, Chem. Eng. J., 2013, 230, 328-337.

[23] L. Yan, Y. B. Zheng, F. Zhao, S. J. Li, X. F. Gao, B. Q. Xu, P. S. Weiss and Y. L. Zhao, Chem. Soc. Rev., 2012, 41, 97–114.

[24] R. L. Liu, D. Q. Wu, X. L. Feng and K. Mullen, J. Am. Chem. Soc., 2011, 133, 15221–15223.

[25] Z. Z. Sun, Z. Yan, J. Yao, E. Beitler, Y. Zhu and J. M.Tour, Nature, 2010, 468, 549-552.

[26] Y. Wang, H. Sun, R. Zhang, S. N. Yu and J. L. Kong, Carbon, 2013, 53, 245-251.

[27] C. Ruiz-Garcia, M. Darder, P. Aranda and E. Ruiz-Hitzky, J. Mater. Chem. A, 2014, 2, 2009–2017.

[28] Sun-Min Jung, E. K. Lee, M. Choi, D. B. Shin, In-Yup Jeon, Jeong-Min Seo, H. Y. Jeong, N. Park, J. H. Ohand and Jong-Beom Baek, Angew. Chem. Int. Ed., 2014, 53, 2398–2401.

[29] J. Gong, J. Liu, X. Wen, Z. W. Jiang, X. C. Chen, E. Mijowska and T. TangInd, Eng. Chem. Res., 2014, 53, 4173–4181.

[30] D. H. Seo, A. E. Rider, Z. J. Han, S. Kumar and K. Ostrikov, Adv. Mater., 2013, 25, 5638–5642.

[31] E. Ruiz-Hitzky, M. Darder, F. M. Fernandes, E. Zatile, F. J. Palomares and P. Aranda, Adv. Mater., 2011, 23, 5250–5255.

[32] S. S. Gupta, T. S. Sreeprasad, S. M. Maliyekkal, S. K. Das and T. Pradeep, ACS Appl. Mater. Interfaces, 2012, 4, 4156–4163.

[33] T. S. Sreeprasad, S. S. Gupta, S. M. Maliyekkal and T. Pradeep, J. Hazard. Mater.,

2013, 246–247, 213–220.

[34] Y. Q. Dong, J. W. Shao, C. Q. Chen, H. Li, R. Wang, Y. W. Chi, X. M. Lin and G. N. Chen, Carbon, 2012, 50, 4738-4743.

[35] Z. F. Tian, C. H. Liang, J. Liu, H. M. Zhang and L. D. Zhang, J. Mater. Chem., 2011, 21, 18242–18247.

[36] M. F. Mangiamelia, J. C. Gonzalez, S. Garcia, S. Bellu, M. Santoro, E. Caffaratti, M. I. Frascaroli, J. M. S. Peregrin, A. M. Atria and L. F. Sala, J. Phys. Org. Chem., 2010, 23, 960–971.

[37] In-Yup Jeon, Yeon-Ran Shin, Gyung-Joo Sohn, Hyun-Jung Choi, Seo-Yoon Bae, J. Mahmood, Sun-Min Jung, Jeong-Min Seo, Min-Jung Kim, D. W. Chang, L. M. Dai and Jong-Beom Baek, Pans, 2012, 109, 5588–5593.

[38] A. Kundu, G. Redzwan, J. N. Sahu, S. Mukherjee, B. S. Gupta and M. A. Hashim, Bioresources, 2014, 9(1), 1498-1518.

[39] Z. A. AL-Othman, R. Ali and M. Naushad, Chem. Eng. J., 2012, 184, 238–247.

[40] M. P. Candela, J. M. Martinez and R. T. Macia, Water Res., 1995, 29(9), 2174-2180.

[41] S. J. Park and W. Y. Jung, Carbon Sci., 2001, 2(1), 15-21.

[42] T. Karthikeyan, S. Rajgopal and L. R. Miranda, J. Hazard. Mater., 2005, B124, 192–199.

[43] N. K. Hamadi, X. D. Chen, M. M. Farid and M. G. Q. Lu, Chem. Eng. J., 2001, 84(2), 95–105.

[44] S. B. Lalvani, T. Wkltowski, A. Hubner, A. Weston and N. Mandich, Carbon,

1998, 36, 1219-1226.

[45] T. H. Liu, Y. H. Li, Q. J. Du, J. K. Sun, Y. Q. Jiao, G. M. Yang, Z. H. Wang, Y. Z. Xia, W. Zhang, K. L. Wang, H. W. Zhu and D. H. Wu, Colloids Surf. B-Biointerfaces, 2012, 90, 197–203.

[46] F. Liu, Y. J. Jin, H. B. Liao, L. Cai, M. P. Tong and Y. L. Hou, J. Mater. Chem. A, 2013, 1, 805–813.

[47] T. Wen, X. L. Wu, M. C. Liu, Z. H. Xing, X. K. Wang and An-Wu Xu, Dalton Trans., 2014, 43, 7464.

[48] L. H. Ai, C. Y. Zhang and Z. L. Chen, J. Hazard. Mater., 2011, 192, 1515–1524.

[49] Ling-wen Xiong, S. H. Liu and Bi-xian Peng, Appl. Opt. 1998, 37, 3678−3684.